Article

Excitation Energy Migration Processes in Cyclic Porphyrin Arrays Probed by Single Molecule Spectroscopy

Jaesung Yang, Mira Park, Zin Seok Yoon, Takaaki Hori, Xiaobin Peng, Naoki Aratani, Peter Dedecker, Jun-ichi Hotta, Hiroshi Uji-i, Michel Sliwa, Johan Hofkens, Atsuhiro Osuka, and Dongho Kim

J. Am. Chem. Soc., **2008**, 130 (6), 1879-1884 • DOI: 10.1021/ja075701b

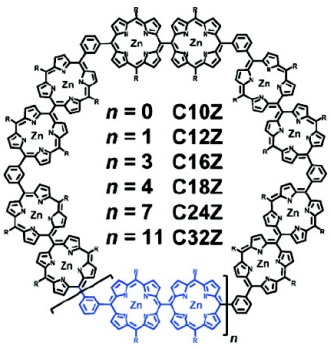

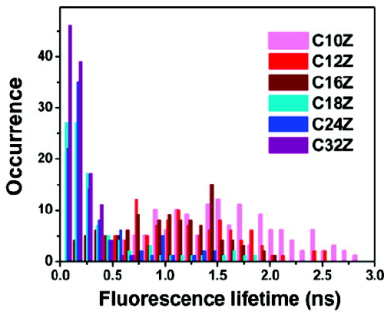

More About This Article

Additional resources and features associated with this article are available within the HTML version:

- Supporting Information
- Links to the 4 articles that cite this article, as of the time of this article download
- Access to high resolution figures
- Links to articles and content related to this article
- Copyright permission to reproduce figures and/or text from this article

View the Full Text HTML

J|A|C|S
ARTICLES
Published on Web 01/18/2008

Excitation Energy Migration Processes in Cyclic Porphyrin Arrays Probed by Single Molecule Spectroscopy

Jaesung Yang,[†] Mira Park,[†] Zin Seok Yoon,[†] Takaaki Hori,[‡] Xiaobin Peng,[‡] Naoki Aratani,[‡] Peter Dedecker,[§] Jun-ichi Hotta,[§] Hiroshi Uji-i,[§] Michel Sliwa,[§] Johan Hofkens,*[,§] Atsuhiro Osuka,*[,‡] and Dongho Kim*[,†]

Center for Ultrafast Optical Characteristics Control and Department of Chemistry, Yonsei University, Seoul 120-749, Korea, Department of Chemistry, Graduate School of Science, Kyoto University, Sakyo-ku, Kyoto 606-8502, Japan, and Department of Chemistry, Katholieke Universiteit Leuven and Institute for Nanoscale Physics and Chemistry (INPAC), Celestijnenlaan 200F, 3001 Heverlee, Belgium

Received July 31, 2007; E-mail: johan.hofkens@chem.kuleuven.ac.be; osuka@kuchem.kyoto-u.ac.jp; dongho@yonsei.ac.kr

Abstract: By using single molecule fluorescence spectroscopy we have investigated the excitation energy migration processes occurring in a series of cyclic porphyrin arrays bearing a close proximity in overall architectures to the LH2 complexes in purple bacterial photosynthetic systems. We have revealed that the conformational heterogeneity induced by the structural flexibility in large cyclic porphyrin arrays, which provides the nonradiative deactivation channels as an energy sink or trap, reduces significantly the energy migration efficiency. Our study provides detailed information on the energy migration efficiency of the artificial light-harvesting arrays at the single molecule level, which will be a guideline for future applications in single molecular photonic devices in the solid state.

Introduction

Inspired by the cyclic arrangement of the strongly interacting 9 BChl a dimeric pigments in B850 of LH2,[1−4] there have been numerous trials in the synthesis of the cyclic porphyrin arrays to pursue the similarities in architectures to the LH1 and LH2 complexes for the fabrication of an artificial light-harvesting apparatus.[5−9] One of the key features in this approach is a fine control of molecular structure because of a close relationship between structure and the photophysical property.[10−17] In this regard, we have synthesized a series of cyclic porphyrin arrays **C10Z**, **C12Z**, **C16Z**, **C18Z**, **C24Z**, and **C32Z**, in which *meso*−*meso* linked Zn(II) diporphyrin (**Z2**) subunits are bridged by 1,3-phenylene linkers (Chart 1).[18−20]

The constituent building block elements of **Z2** are similar to the BChl a dimeric pigments in B850 of LH2. Especially, the cyclic porphyrin array **C18Z** possesses a close proximity in overall structure to the B850 of LH2 complexes.

In recent years single molecule fluorescence spectroscopy (SMFS) at room temperature has been extensively used to investigate the molecular distribution of physical quantities rather than the ensemble-averaged values from the bulk measurements. By using SMFS, we can obtain direct information on the chemical and spectroscopic heterogeneities of single molecules[21,22] as well as the dynamics of these heterogeneities.[23] However, the multichromophoric systems composed of porphyrin molecules have scarcely been studied by SMFS due to their inherent low fluorescence quantum yields. Despite this, it is crucial to examine the photophysical properties of porphyrin-

[†] Yonsei University.
[‡] Kyoto University.
[§] Katholieke Universiteit Leuven and Institute for Nanoscale Physics and Chemistry (INPAC).

(1) Roszak, A. W.; Howard, T. D.; Southall, J.; Gardiner, A. T.; Law, C. J.; Issac, N. W.; Cogdell, R. J. *Science* **2003**, *302*, 1969.
(2) McDermott, G.; Prince, S. M.; Freer, A. A.; Hawthonthwaite-Lawless, A. M.; Papiz, M. Z.; Cogdell, R. J.; Isaacs, N. W. *Nature* **1995**, *374*, 517.
(3) Freer, A. A.; Prince, S. M.; Sauer, K.; Papiz, M. Z.; Hawthonthwaite-Lawless, A. M.; McDermott, G.; Cogdell, R. J.; Isaacs, N. W. *Structure* **1996**, *4*, 564.
(4) Jungas, C.; Ranck, J.; Rigaud, J.; Joliot, P.; Vermeglio, A. *EMBO J.* **1999**, *18*, 534.
(5) Anderson, H. L.; Sanders, J. K. M. *J. Chem. Soc., Chem. Commun.* **1989**, 1714.
(6) Biemans, H. A. M.; Rowan, A. E.; Verhoeven, A.; Vanoppen, P.; Latterini, L.; Foekema, J.; Schenning, A. P. H. J.; Meijer, E. W.; De Schryver, F. C.; Nolte, R. J. M. *J. Am. Chem. Soc.* **1998**, *120*, 11054.
(7) Li, J.; Ambroise, A.; Yang, S. I.; Diers, J. R.; Seth, J.; Wack, C. R.; Bocian, D. F.; Holten, D.; Lindsey, J. S. *J. Am. Chem. Soc.* **1999**, *121*, 8927.
(8) Drain, C. M.; Nifiatis, F.; Vasenko, A.; Batteas, J. D. *Angew. Chem., Int. Ed.* **1998**, *37*, 2344.
(9) Kato, A.; Sugiura, K.; Miyasaka, H.; Tanaka, H.; Kawai, T.; Sugimoto, M.; Yamashita, M. *Chem. Lett.* **2004**, *33*, 578.
(10) Anderson, S.; Anderson, H. L.; Sanders, J. K. M. *Acc. Chem. Res.* **1993**, *26*, 469.
(11) Imamura, T.; Fukushima, K. *Coord. Chem. Rev.* **2000**, *198*, 133.
(12) Satake, A.; Kobuke, Y. *Tetrahedron* **2005**, *61*, 13.
(13) Wojaczynski, J.; Latos-Grazynski, L. *Coord. Chem. Rev.* **2000**, *204*, 113.
(14) Iengo, E.; Zangrando, E.; Alessio, E. *Eur. J. Inorg. Chem.* **2003**, 2371.
(15) Brodard, P.; Matzinger, S.; Vauthey, E.; Mongin, O.; Papamicaël, C.; Gossauer, A. *J. Phys. Chem. A* **1999**, *103*, 5858.
(16) Takahashi, R.; Kobuke, Y. *J. Am. Chem. Soc.* **2003**, *125*, 2372.
(17) Wasielewski, M. R. *Chem. Rev.* **1992**, *92*, 435.
(18) Peng, X.; Aratani, N.; Takagi, A.; Matsumoto, T.; Kawai, T.; Hwang, I.-W.; Ahn, T. K.; Kim, D.; Osuka, A. *J. Am. Chem. Soc.* **2004**, *126*, 4468.
(19) Hori, T.; Aratani, N.; Takagi, A.; Matsumoto, T.; Kawai, T.; Yoon, M.-C.; Yoon, Z. S.; Cho, S.; Kim, D.; Osuka, A. *Chem.*−*Eur. J.* **2006**, *12*, 1319.
(20) Park, M.; Yoon, M.-C.; Yoon, Z. S.; Hori, T.; Peng, X.; Aratani, N.; Hotta, J.; Uji-i, H.; Sliwa, M.; Hofkens, J.; Osuka, A.; Kim, D. *J. Am. Chem. Soc.* **2007**, *129*, 3539.
(21) Macklin, J. J.; Trautman, J. K.; Harris, T. D.; Brus, L. E. **1996**, *272*, 255.
(22) Lu, H. P.; Xie, X. S. *J. Phys. Chem. B* **1997**, *101*, 2753.
(23) Ha, T.; Enderle, T.; Chemla, D. S.; Selvin, P. R.; Weiss, S. *Phys. Rev. Lett.* **1996**, *77*, 3979.

Chart 1. Molecular Structures of a Series of Cyclic Porphyrin Arrays[a]

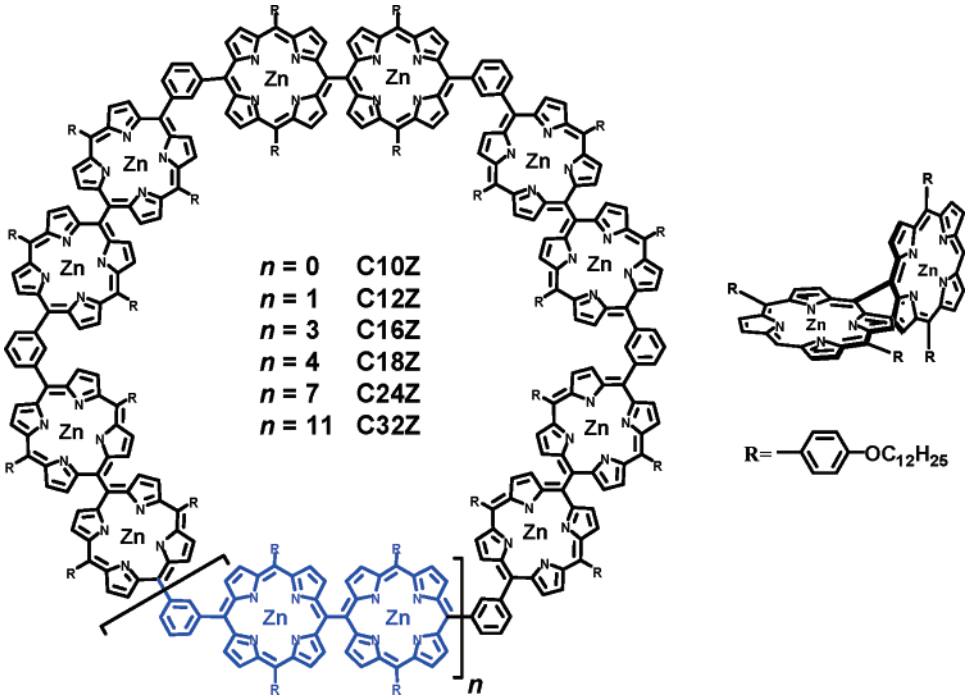

[a] The cyclic porphyrin arrays are composed of *meso*−*meso* directly linked Zn(II) diporphyrin subunits **Z2** bridged by 1,3-phenylene spacers.

based molecular systems at the single molecule level not only to directly observe salient behaviors of individual molecules but also for the practical purpose to fabricate the artificial light-harvesting complexes in solid state.

In this work, the fluorescence properties of the cyclic porphyrin arrays have been comparatively investigated by SMFS with a particular focus on the influences of the overall structural rigidity on the excitation energy migration as the size of a cyclic porphyrin array becomes larger. Survival times in fluorescence intensity trajectories, relative molecular brightness, fluorescence decays, and interphoton arrival time distributions were measured at the single molecule level. Our results obtained from these spectroscopic investigations on single molecules provide detailed information on the excitation energy migration efficiency in the solid state.[24−29]

Experimental Section

Sample Preparation. The synthesis of cyclic porphyrin arrays studied here was performed by the intramolecular Ag(I)-promoted cyclization reaction, which was reported previously for **C12Z**.[5−6] The synthetic details of the other arrays will be reported elsewhere. Samples for single molecule measurements were prepared by spin-coating (2000 rpm) of a solution of a cyclic porphyrin array ($\sim 10^{-10}$ M) in chloroform (Aldrich, spectrophotometric grade) containing 2−5 mg/mL poly (methyl methacrylate) (PMMA) on rigorously cleaned cover glasses. The optical density of the sample solution was measured to determine the concentration.

Ensemble Spectroscopy. Steady-state absorption spectra were recorded by using a UV−vis spectrometer (Varian, model Cary5000), and steady-state emission spectra were recorded by using a fluorometer (Hitachi, model F-2500). The fluorescence quantum yields were obtained compared with the fluorescence quantum yield of ~0.03 of a zinc(II) tetraphenylporphyrin as a reference with the excitation wavelength of 550 nm. The time-correlated single photon counting (TCSPC) system was used for the fluorescence decay measurement. The system consisted of a self-mode locked and cavity-dumped femtosecond Ti: sapphire laser pumped by a continuous wave (cw) Nd:YAG laser (Coherent, Verdi). The full width at half-maximum of the instrument response function of 60 ps was obtained. The fluorescence decays were measured with magic-angle emission polarization, and the number of fluorescence photons per unit time was always maintained at <1% of the repetition rate of the excitation pulses to prevent pile-up distortions in the decay profiles.

Single Molecule Spectroscopy. To determine the single-molecule survival times and fluorescence brightnesses a laser scanning confocal microscope system based on an inverted type optical microscope was used for fluorescence detection of a single molecule. The sample scanning was achieved by using an $x-y$ scanning sample stage consisting of two electrostrictive actuators (AD-100, New Port) and a two-axis linear translator stage. The excitation laser beam at 543.5 nm from a He−Ne laser (25 LGR 193-230, Melles Griot) was delivered to the input port of the confocal microscope through a single-mode optical fiber. The laser beam from the fiber was filtered by a narrow-band interference filter (F10-546.1-4-1.00, CVI Laser Corp.) and then reflected up to the microscope objective lens (Plan-neofluar 100× oil immersion, Carl Zeiss) by using a dichroic beam splitter (565DCXR, Chroma). The laser beam was expanded to 10 mm in diameter before it impinged on the excitation filter to get higher optical resolution. The fluorescence of single molecules was collected by the same microscope objective lens and focused through a 150 mm focal length lens onto an APD detector in a single photon counting mode (SPCM-AQR-14-FC, EG&G, Perkin-Elmer Optoelectronics, Norwalk, CT). Scattered light around the excitation wavelength was removed by placing a suitable filter between the objective lens and the focusing lens. The electrical pulses from the output of an APD detector were counted with a computer plug-in counter board (PCI 6602, National Instruments).

(24) Gust, D.; Moore, T. A.; Moore, A. L. *Acc. Chem. Res.* **2001**, *34*, 40.
(25) Holten, D.; Bocian, D. F.; Lindsey, J. S. *Acc. Chem. Res.* **2002**, *35*, 57.
(26) Kim, D.; Osuka, A. *Acc. Chem. Res.* **2004**, *37*, 735.
(27) Prodi, A.; Chiorboli, C.; Scandola, F.; Iengo, E.; Alessio, E.; Dobrawa, R.; Würthner, F. *J. Am. Chem. Soc.* **2005**, *127*, 1454.
(28) Wagner, R. W.; Lindsey, J. S. *J. Am. Chem. Soc.* **1994**, *116*, 9759.
(29) Debreczeny, M. P.; Svec, W. A.; Wasielewski, M. R. *Science* **1996**, *274*, 584.

Sample stage scanning and data acquisition were controlled by a personal computer based on a visual basic program. While scanning the cover glasses to locate individual molecules we introduced an additional neutral-density filter in the beam path to reduce the probability of photobleaching occurring during this scanning. For fluorescence decay measurements, the excitation light of 568 nm (8.18 MHz repetition rate, 1.2 ps full width at half-maximum) from the frequency doubled output of an optical parametric oscillator (GWU) pumped by a Ti:Sapphire laser (Tsunami, Spectra Physics) was rendered circularly polarized by a Berek compensator, directed into an inverted microscope (Olympus IX 70), and focused onto the sample through an oil immersion objective (1.3 NA, 100×, Olympus). Fluorescence was collected through the same objective and focused onto an avalanche photodiode (SPCM 15, EG&G). Time-resolved data were collected with a TCSPC card (SPC 630, Becker & Hickl) operated in the First-in-first-out mode. This combination of the card used in the FIFO mode and the APD allows one to get the fluorescence signal and the decay profile of single molecules with an experimental instrument response on the order of 400 ps. The maximum likelihood estimation (MLE) method was used to analyze the single molecule fluorescence decays.[30] The detailed description of the setup and the data acquisition process has been published previously.[31]

For coincidence measurements, a classical Hanbury-Brown and Twiss antibunching setup was used.[32] In the confocal microscope described above, the fluorescence from a single molecule was split by a 50:50 nonpolarizing beam splitter and detected by two APDs. The signal from both APDs was fed into the router coupled to the TCSPC acquisition card. Because the TCSPC card has a dead time of 125 ns, an electronic delay is applied to the signal of one of the two APDs, so that multiple fluorescence photons generated by the same laser pulse can be detected. The TCSPC card registers for both APDs the arrival time after the beginning of the acquisition with a resolution of 50 ns (a, macro-time) and the time delay between the start pulse (fluorescence) and stop pulse (laser) with a time resolution of 6 ps (b, micro-time). The electronic delay was set to 1.44 s. Histograms of interphoton arrival times were obtained by combining micro-times and macro-times using the timing of the laser pulse with a home made program in visual C++.

Results and Discussion

Distribution of Survival Times. In SMFS, the survival time corresponds to the time span between the start of the fluorescence intensity trajectory (FIT) and the decrease of the fluorescence emission to the background level due to irreversible photobleaching. Thus, the survival time in FIT is related to the number of chromophores in a multichromophoric system. Figure 1 shows the distribution of survival times and the plot of mean survival times of ~100 cyclic porphyrin array molecules embedded in a PMMA matrix. The mean value of survival times in FITs gradually increases as the number of porphyrin units in the cyclic porphyrin array increases.

Moreover, the survival time distribution of the largest cyclic porphyrin array **C32Z** is seen to be relatively broader compared to the other cyclic porphyrin arrays. This can be explained by realizing that the larger ring structure of **C32Z** has more conformational flexibility than the smaller arrays. This indicates the existence of conformational heterogeneity in larger cyclic arrays and that the extent of the conformational heterogeneity increases as the cyclic porphyrin array becomes larger. The conformational heterogeneities in larger porphyrin arrays are

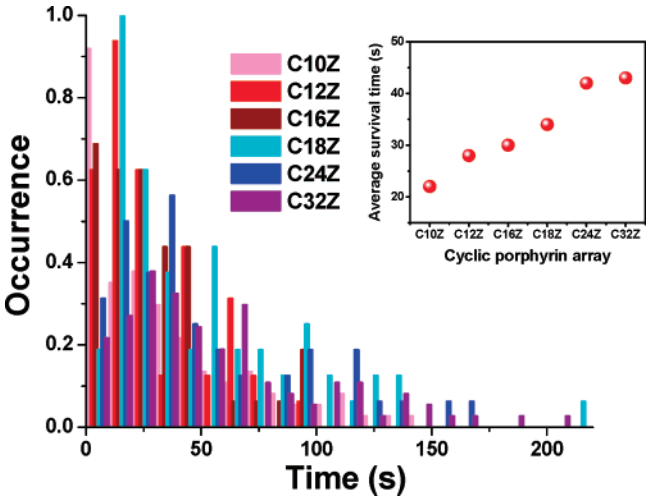

Figure 1. Distribution of survival times in the cyclic porphyrin arrays **C10Z**, **C12Z**, **C16Z**, **C18Z**, **C24Z**, and **C32Z**. The inset represents the plot of mean value of survival times.

believed to arise from the dihedral and tilting angle distribution between the adjacent subunits, porphyrin dimers, induced by the summation of angle changes between 1,3-phenylene spacers.

In FITs, as the cyclic porphyrin array becomes larger, the occurrence of the single-step photobleaching process decreases in favor of multistep photobleaching: ~15% of 218 molecules for **C10Z**, ~18% of 140 molecules for **C12Z**, ~8% of 100 molecules for **C16Z**, ~5% of 120 molecules for **C18Z**, and ~3% of 99 molecules for **C24Z** show single-step photobleaching (Figure S4a). In the largest cyclic porphyrin array **C32Z**, none of 110 molecules investigated exhibits the single-step photobleaching in FITs. In small cyclic porphyrin arrays, the high occurrence of single-step photobleaching can be understood as a generation of an exciton trap by photobleaching. Once the trap is formed the efficient energy migration within the cyclic porphyrin array permits the excited states to be quenched nonradiatively by the trap. In contrast, in large cyclic porphyrin arrays, the high occurrence of multiple-step photobleaching, of which the majority includes off-times, in FITs is suggested to be the result of less efficient energy migration along the cyclic array to the trapping site due to the distortion of the ring structure in large cyclic arrays. Furthermore, in addition to the conformational heterogeneity a relatively large ring size itself probably makes it difficult for the single trap to quench all of the excitation energies.

Fluorescence Decays. To examine the excited-state dynamics of the cyclic porphyrin arrays, we measured the fluorescence decays in ensemble (toluene and bulk PMMA film) and at the single molecule level by using the time-correlated single photon counting method. The fitted fluorescence lifetimes are tabulated (Table 1).

In the ensemble fluorescence decay profiles in PMMA film and toluene (Figure S3), the average fluorescence lifetime decreases as the cyclic porphyrin array becomes larger, up to the largest cyclic porphyrin array **C32Z**. In relatively small cyclic porphyrin arrays **C10Z** and **C12Z**, the fluorescence decay profiles show single exponential decay. On the other hand, in larger cyclic porphyrin arrays than **C12Z**, the fluorescence temporal profiles start to show double exponential decay. The contribution by the fast decay component in double exponential decay increases as the cyclic porphyrin arrays become larger.

(30) Maus, M.; Cotlet, M.; Hofkens, J.; Gensch, T.; De Schryver, F. C.; Schaffer, J.; Seidel, C. A. M. *Anal. Chem.* **2001**, *73*, 2078.
(31) Vosch, T.; Cotlet, M.; Hofkens, J.; Van Der Biest, K.; Lor, M.; Weston, K.; Tinnefeld, P.; Sauer, M.; Latterini, L.; Mullen, K.; De Schryver, F. C. *J. Phys. Chem. A* **2003**, *107*, 6920.
(32) Hanbury-Brown, R.; Twiss, R. Q. *Nature* **1956**, *177*, 27.

Table 1. Fluorescence Lifetimes of Cyclic Porphyrin Arrays Depending on Experimental Conditions

	fluorescence decay times (ns) and relative amplitude (%)		
cyclic array	in solution[a]	in bulk film[b]	at single molecule[c]
C10Z	1.73	1.69	1.58
C12Z	1.54	1.51	1.23
C16Z	0.07 (55)/1.6 (45)	0.10 (51)/1.4 (49)	0.84
C18Z	0.06 (69)/1.6 (31)	0.13 (66)/1.3 (34)	0.42
C24Z	0.13 (75)/1.5 (25)	0.18 (71)/1.2 (29)	0.32
C32Z	0.19 (79)/1.5 (21)	0.16 (85)/1.1 (15)	0.16

[a] The solvent used was toluene. The excitation wavelength of 400 nm and emission wavelength of 650 nm were applied. [b]Bulk film samples were prepared by spin-coating of a solution of the cyclic porphyrin array (10^{-7}–10^{-8} M) in chloroform containing 5 mg/mL PMMA polymer matrix on cleaned cover glasses. [c]Average fluorescence lifetimes of single cyclic porphyrin array molecules, according to all the counts at the initial emission level in fluorescence intensity trajectory.

We attribute the fast picosecond component in the larger arrays to the presence of conformations with additional nonradiative decay paths, such as kink structures. In contrast, the slow decay component may be caused by those conformations that have well-defined and rigid structures.

Figure 2a shows a distribution of the fluorescence decays corresponding to all the detected photons at the initial emission level in FITs of the cyclic porphyrin arrays, and Figure 2b shows a typical FIT and fluorescence decay for a single molecule of cyclic porphyrin array **C18Z**, illustrating the fluorescence decay at the initial emission level in FIT. We have also added several FITs for single **C12Z** molecules as Figure S3 in the Supporting Information. We could describe these decays using only a single-exponential term, though the limited amount of photons in single-molecule FITs means that we cannot reliably detect the presence of an additional decay term with a low relative contribution. In the fluorescence lifetime distributions, the mean fluorescence lifetime of **C16Z** is 0.84 ns with a much wider distribution ranging from 0.2 to 2.6 ns compared to the smaller cyclic porphyrin arrays. This relatively large spread can be explained by the larger conformational freedom and, hence, larger conformational heterogeneity of the larger ring structure. In contrast, in the larger cyclic porphyrin arrays **C18Z**, **C24Z**, and **C32Z**, the distribution of fluorescence lifetimes becomes narrow with a significant reduction in their lifetimes. This is consistent with the ensemble data, where the fast decay constant becomes increasingly dominant as the size of the porphyrin arrays is increased.

Fluorescence Quantum Yields. The decrease of fluorescence quantum yields in a series of cyclic porphyrin arrays shows a good correlation with the double exponential fluorescence decay abruptly appearing from **C16Z**. Figure 3 shows the plot of relative molecular brightness and relative fluorescence quantum yields in the cyclic porphyrin arrays at the single molecule level and in solution, respectively.

The red circles indicate the mean value of relative molecular brightness of 300 individual cyclic porphyrin arrays, respectively. The relative molecular brightness in a single molecule can be estimated by the initial fluorescence intensity in FIT and the extinction coefficient. The initial fluorescence intensity in FIT is related to the probability to emit fluorescence via absorption in a cyclic porphyrin array. Therefore, the relative molecular brightness at the single molecule level corresponds to the initial fluorescence intensity divided by the extinction coefficient in the cyclic porphyrin array. In a series of cyclic

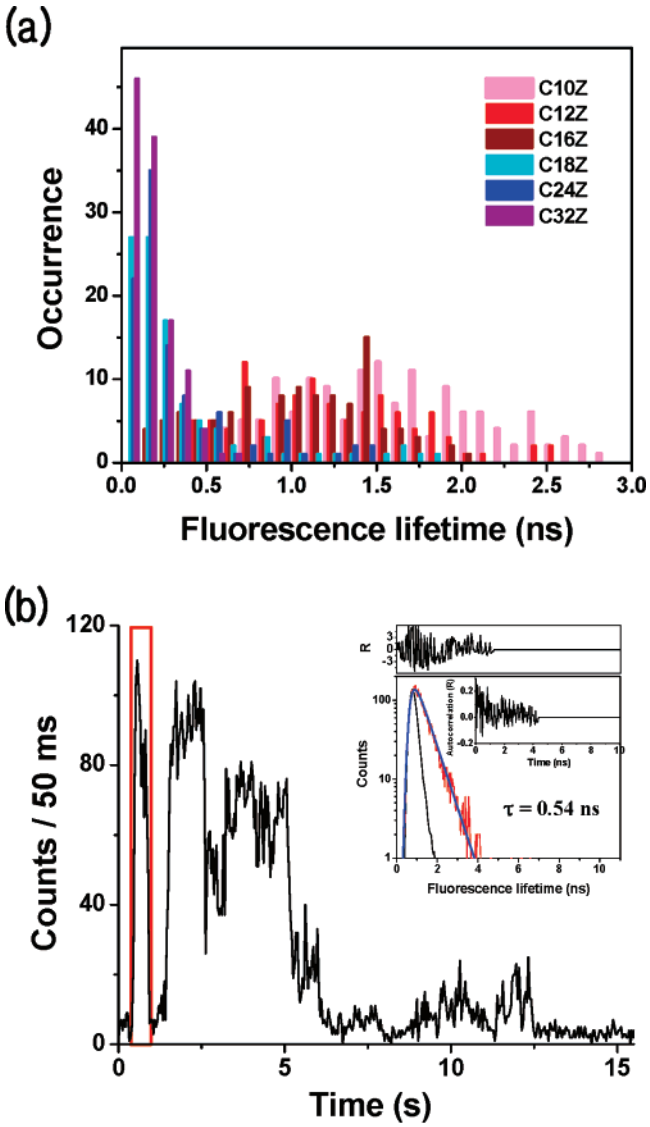

Figure 2. Time-resolved fluorescence decay measurements on a single molecule for the cyclic porphyrin arrays **C10Z**, **C12Z**, **C16Z**, **C18Z**, **C24Z**, and **C32Z**. Histogram of the decay values obtained from single cyclic porphyrin array molecules (a). A fluorescence intensity trajectory (FIT) of a single **C18Z** molecule in PMMA film. Fluorescence decay and fit corresponding to the initial emission level in the FIT. The region corresponding to the decay is colored in red (b).

porphyrin arrays, the molar extinction coefficients as a function of the number of porphyrin dimer units exhibit a linear behavior, indicating the higher absorptivity as the cyclic porphyrin array becomes larger (Figure S2). The initial fluorescence intensity also increases in large cyclic porphyrin arrays due to the increase in the number of chromophore units. For **C10Z** and **C12Z**, the average count rate in the initial emission level increases from 2200 to 3900 s^{-1}, and the extinction coefficient also increases from 1.59×10^5 to 2.06×10^5 M^{-1} cm^{-1}. As a dimer subunit in the cyclic porphyrin array is added from **C10Z** to **C12Z**, the relative molecular brightness increases by about 16%. On the other hand, in larger cyclic arrays than **C12Z**, the relative molecular brightness gradually decreases, because the count rate at the initial emission level does not increase linearly. Thus, the relative molecular brightness in the cyclic porphyrin arrays reach a maximum value at **C12Z** and then decrease as the cyclic porphyrin array become larger than **C12Z**. This is consistent

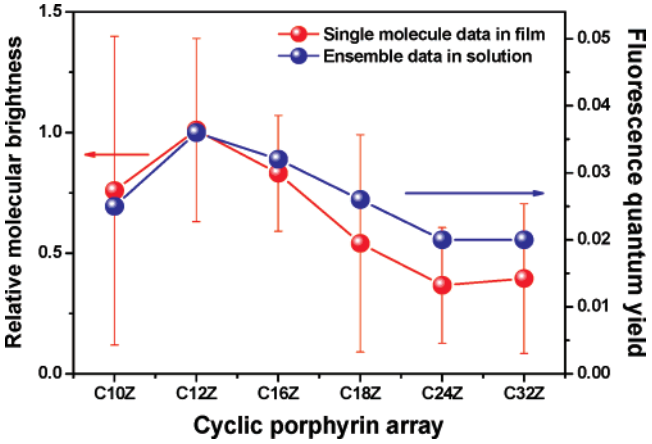

Figure 3. Plot of average values of the relative molecular brightness at the single molecule level and fluorescence quantum yields in toluene in the cyclic porphyrin arrays. The error range indicates the standard deviation of the relative molecular brightness for each cyclic porphyrin array.

with the ensemble-level fluorescence quantum yields, as well as the very short excited-state lifetimes for the larger cyclic arrays. Therefore, we similarly attribute this to the presence of more conformational heterogeneity as the cyclic porphyrin arrays become larger than **C12Z**, which leads to the reduction of the fluorescence quantum yield.

In Figure 3, the relative molecular brightness at the single molecule level is lower than relative fluorescence quantum yield in solution in the large cyclic porphyrin arrays. This can be explained by a difference in the degree of freedom in the surrounding environment of the cyclic porphyrin arrays between solution and a polymer matrix.

Coincidence Measurements. We have tried to evaluate the energy migration efficiency via singlet−singlet (S_1-S_1) annihilation processes as the number of dimer subunits in the cyclic porphyrin array increases. Coincidence measurements were carried out on single molecules of **C10Z**, **C12Z**, and **C16Z** to estimate the energy migration efficiency via an S_1-S_1 annihilation process when a molecule was excited with relatively intense laser pulses. The S_1-S_1 annihilation provides information about the energy migration within the cyclic porphyrin array, in which the S_1-S_1 annihilation can be understood in terms of two or more singlet excitons formed by the sequential absorption, within one laser pulse, of at least two photons in a cyclic porphyrin array. The two or more singlet excitons quickly relax to the ground state to produce higher excited exciton through collisional process mediated by sequential energy migration along the cyclic array ($S_1 + S_1 \rightarrow S_o + S_n$), in which the higher excited exciton relaxes to the S_1 state via fast internal conversion process. Consequently, the observed number of S_1 fluorescence photons is a direct indication of the efficiency of Förster-type energy transfer among excited dimer subunits in the cyclic porphyrin array.

The number of excitations per laser pulse can be calculated at the single molecule level as follows: the absorption cross section (σ) of **C10Z** is calculated to be 5.74×10^{-16} cm^2 by the extinction coefficient (ϵ) 1.50×10^5 M^{-1} cm^{-1} at 568 nm. The average power of 4 μW with a repetition rate of 8.13 MHz corresponds to 4.92×10^{-13} J/pulse. One photon of 568 nm light has an energy of 3.50×10^{-19} J corresponding to 1.41×10^6 photons per pulse. The photon density in the focused beam diameter of 3.41×10^{-10} cm^2 is 4.13×10^{15} photons/cm^2. As a consequence, two porphyrins in a cyclic porphyrin array can be simultaneously excited per laser pulse.

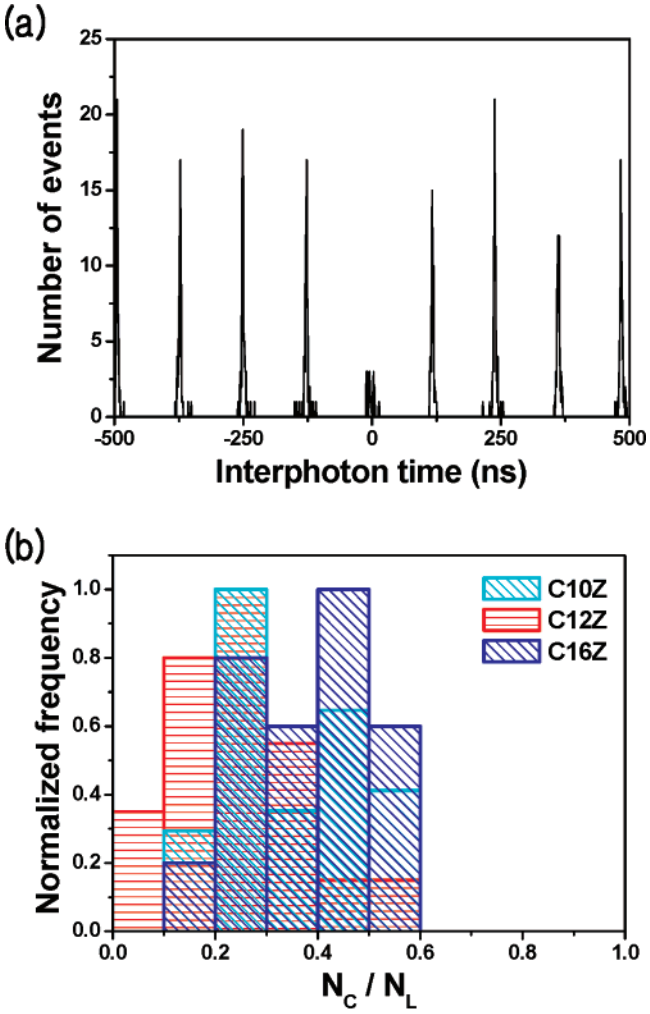

Figure 4. Coincidence measurements on a single molecule for the cyclic porphyrin arrays **C10Z**, **C12Z**, and **C16Z**. Interphoton arrival time distribution in the coincidence measurements obtained for **C12Z** (a). The histogram of N_C/N_L values of single **C10Z**, **C12Z**, and **C16Z** molecules. The mean value of N_C/N_L ratios for **C10Z**, **C12Z**, and **C16Z** are 0.34, 0.24, and 0.38, respectively (b).

Interphoton arrival time distribution taken from the first emissive level in the FIT of **C12Z** is shown in Figure 4a.

The central peak (N_C) around 0 ns corresponds to photon pairs by the same laser pulse. In all other cases, interphoton arrival times are distributed in lateral peaks (N_L), which appear every 123 ns corresponding to a multiple of the laser repetition period. It should be noted that the central peak can also be observed by a few accidental coincidences, which are attributed to background−background, background−signal, and signal−background photon pairs. The distribution shown in Figure 4a exhibits a very small central peak compared to lateral peaks, which is commonly observed for a single-photon emitting system, indicating that singlet−singlet annihilation readily occurs in **C12Z** by efficient excitation energy migration process.

Histograms for the ratio of the number of photons in the central peak to the number of photons averaged from 34 lateral peaks of individual **C10Z**, **C12Z**, and **C16Z** molecules are displayed in Figure 4b. The N_C/N_L ratio in the coincidence measurements can be used to estimate the number of emitting

porphyrin units in the multichromophoric arrays, with a value of 0 corresponding to a single-photon emitter and 0.5 to a two-photon emitter. Larger values suggest even less efficient S_1-S_1 annihilation processes.

The mean N_C/N_L values of **C10Z** and **C16Z** are 0.34 and 0.38, respectively, which are larger than the value of 0.24 found for **C12Z**. At the same time, we could only find N_C/N_L ratios below 0.1 for **C12Z** and not for **C10Z** or **C16Z**. We attribute the less efficient annihilation in **C10Z** to the considerable structural strain that can occur due to the smaller ring size as compared with **C12Z**, giving rise to a change in dihedral angle and orientation factor between dimer subunits. For the Förster resonance energy transfer (FRET) processes, this enforced strain may disturb the exciton delocalization by perturbing dipole−dipole coupling between dimer subunits. The less efficient S_1-S_1 annihilation in **C16Z** is presumably due to the presence of less-favorable structural conformations as well as the longer average interchromophoric distance between dimer subunits via the 1,3-phenylene spacer as compared with **C12Z**. The relatively smaller N_C/N_L value of 0.24 for **C12Z** illustrates that **C12Z** can be considered as a well-defined cyclic structure for efficient FRET due to stronger dipole−dipole coupling between porphyrin dimer subunits. Thus, the construction distortion, induced by a change in interchromophoric distance and orientation factor between two transition dipoles of the adjacent dimer subunits in the cyclic porphyrin array, may reduce the energy migration efficiency by disturbing the exciton delocalization.

Conclusions

We have investigated the energy migration processes occurring in a series of cyclic porphyrin arrays as the number of dimer subunits increases systematically at the single molecule level using confocal fluorescence microscopy. Based on our single molecule spectroscopic measurements, we can demonstrate that **C12Z** exhibits the most efficient energy migration process among all the cyclic porphyrin arrays studied here. The 1,3-phenylene spacer with an angle of 120° between the two linking C−C bonds at 1 and 3 positions of the phenyl group is relatively well-suited to accommodate the six porphyrin dimer subunits to form the hexagonal form of the cyclic porphyrin array **C12Z** without a significant distortion in overall structures as compared with the other cyclic porphyrin arrays: either smaller **C10Z** or larger **C16Z**, **C18Z**, **C24Z**, and **C32Z** rings. Thus, in the fabrication of a single molecular light-harvesting device not only the increase in the number of chromophores but also the maintenance of rigid cyclic structures is crucial in the optimization of excitation energy migration efficiency.

Acknowledgment. This research was financially supported by the Star Faculty Program from the Ministry of Education and Human Resources Development of Korea (D.K.). M.P., J.Y., and Z.S.Y. acknowledge the fellowship of the BK21 program from the Ministry of Education and Human Resources Development. The work at Kyoto was supported by the CREST (A.O.). Financial support from the KULeuven research fund (GOA 2/06, Center of Excellence INPAC) and the Federal Science Policy of Belgium (Grant IUAP-VI) is also acknowledged. This work, as part of the European Science Foundation EUROCORES Program SONS, was supported from funds by the FWO and EC Sixth Framework Program, under Contact No. ERAS-CT-2003-980409.

Supporting Information Available: Four additional figures with discussion. This material is available free of charge via the Internet at http://pubs.acs.org.

JA075701B